Title	ROC dependent event isolation method for image processing based assessment of corroded harbour structures
Authors(s)	Pakrashi, Vikram; Schoefs, Franck; Memet, Jean Bernard; O'Connor, Alan
Publication date	2008-04-30
Publication information	Structure and Infrastructure Engineering, 6 (3): 365-378
Publisher	Taylor & Francis
Item record/more information	http://hdl.handle.net/10197/10495
Publisher's statement	This is an Accepted Manuscript of an article published by Taylor & Francis in Structure and Infrastructure on 30 April 2008, available online: http://www.tandfonline.com/10.1080/15732470701718072
Publisher's version (DOI)	10.1080/15732470701718072

ROC Dependent Event Isolation Method for Image Processing Based Assessment of Corroded Harbour Structures

Vikram Pakrashi[a], Franck Schoefs[b], Jean Bernard Memet[c] and Alan O' Connor[a]

[a] **Department of Civil, Structural and Environmental Engineering, Trinity College Dublin, Ireland**

[b] **Institute in Civil and Mechanical Engineering, Nantes Atlantic University, Nantes, France**

[c] **A-Corros expertise, Corrosion and conservation of Cultural heritage, Arles, France**

Abstract: The localisation and calibration of damage in a structure are often difficult, time consuming, subjective and error prone. The importance of a simple, fast and relatively inexpensive non-destructive technique (NDT) with reliable measurements is thus greatly felt. The usefulness and the efficiency of any such technique are often affected by environmental conditions. The definition of damage and the subsequent interpretation of the possible consequences due to the damage introduce subjectivity into an NDT technique and affect its performance. It is of great importance in terms of practical application to find out the efficiency of an NDT technique in a probabilistic way for various damage definitions and environmental conditions through the use of receiver operating characteristic (ROC) curves. Such variations of performance of an NDT tool can be predicted through simulation processes and the test conditions conducive to good detections can be isolated and ranked according to their relative efficiency. This paper considers a camera based image analysis technique to identify, quantify and classify damage in structures at various levels of scale. The general method has been applied to identify the affected areas on aluminium due to pitting corrosion. The method depends on the optical contrast of the corroded region with respect to its surroundings, performs intelligent edge detection through image processing techniques and computes each affected and closed region to predict the total area of the affected part along with its spatial distribution on a two dimensional plane. The effects of various environmental factors on the quality of such images are simulated from an original photograph. The objectivity and the amount of available information, quantification and localisation and the extent of pitting corrosion are observed along with the various constructed ROC curves. The method provides the engineer, the owner of the structure and the end user of

the NDT technique with a tool to assess the performance of the structure in an as-built condition and decide on the appropriateness of a certain NDT under a given environmental condition and a certain definition of damage. Moreover, it allows introducing the findings of the NDT results in the decision chain and in risk analysis.

KEY WORDS: NDT, Image Processing, ROC, Structural Health Monitoring, Maintenance

Correspondence to: Dr. Alan O' Connor, Department of Civil, Structural and Environmental Engineering, Trinity College Dublin, Ireland

E-mail: alan.oconnor@tcd.ie

1. INTRODUCTION

The need of structural health monitoring and assessment using non destructive techniques (NDT) are of great importance in the recent times. The oncoming load, the material properties and geometry have changed significantly in many structures around the world over a period of time since they were built. As these structures are a part (sometimes, a key part) of a larger infrastructure network, they play a major role in terms of facilitating economic activities and trade (SAMARIS, 2005). Thus, for both existing and burgeoning economic zones of importance it is of great interest of the structure owners, managers and end users to be informed about the state of the structure in its as built condition. Although many NDTs have been developed over a few decades, the prime and practical concerns around such techniques revolve around the parameters, the location and the time instants/ intervals of the measurements to obtain a correct and objective quantification of the structure.

Since there is uncertainty related to any NDT method, the efficiency of the method can be expressed appropriately in a probabilistic fashion in terms of the receiver operating characteristic (ROC) curves. Such curves, when available for various governing factors can also act as a sensitivity study and help ranking different NDTs, or environmental conditions to obtain more correct results in terms of structural assessment. As a result, such a study can identify and isolate the conditions of the operation of an NDT tool while simultaneously quantifying its performance.

A specific example of the need of isolating the operating conditions and quantifying the performance of an NDT tool has been felt in recent past during the assessment of a metallic pile wharf located at St. Nazaire, a very important harbour on the Atlantic side of France in the estuary of Loire river between Nantes and Saint Nazaire towns. Being in the marine environment, the metallic piles are susceptible to many corrosion forms among which pitting corrosion is deemed to be the worst one since the damage usually progresses deep into the metal and not onto the surface as for uniform corrosion. Such corrosion can lead to the damage of the reinforced concrete inside the pile or to the leakage of embankment for sheet piles.

There exist a few indices of determining the presence of this type of corrosion. One of the most efficient is the presence, at the metal surface, of a rust coloured bubble which is visible even if there is fouling on the metal. The health assessment of such a structure is considered to be of great practical importance but the assessment and the quantification of these defects are non-trivial.

In order to assess the damage with respect to time, the owners and the end-users use many NDT techniques such as ultra-sonic (US) measurements to obtain the loss of

thickness, a powerful parameter for damage description. However, the US measurements are essentially local events.

Divers, who are responsible for carrying out the experiments for the inspection and health monitoring of structures are usually provided with a pre-listed guideline indicating the locations for carrying out such experiments. Unfortunately, the guidelines are often set out by the authorities who do not have prior information about the condition of the structures. So the probability of detection of a damage of high extent with possible potential for even larger effects (especially pitting corrosion) is low. Under these circumstances, an image processing based damage detection technique can be a powerful tool for NDT testing in harbour structures before running the US measurements, with the aim of selecting the appropriate zones to be assessed.

Submarine inspections and investigations of localized corrosion have been observed by divers in the site of St. Nazaire in addition to the ultra-sonic measurements. The recorded video tapes and photographs in the inspection report form the basis of identification of the damage conditions on the structure in an as built condition. However, the quality of the videotapes had been extremely poor and it was not possible to identify the damage quantitatively. The necessity of the isolation of operating conditions, NDT rating and interpretation definition directly follow from this practical inability to detect the damage.

Image processing based damage detection and calibration has been very recently successfully used as an NDT tool in various structural health monitoring problems. Patsias and Staszewski (2002) have identified vibration parameters from a video camera based detection system in conjunction with wavelet analysis. Open crack in statically

loaded simply supported beam has been identified using image processing and wavelet analysis by Rucka and Wilde (2006). Hartman and Gilchrist (2004) have employed a video camera based detection of the fatigue of asphalt. Application of such video camera based work has also been seen to track the motion of a cable (Gehle & Masri (1998)). Multiple cameras have been used to identify damages by using photogrammetric software by Benning et.al (2004). Image analysis based identification of human lip from photographs has been performed by Barinova and Pospisil (2002). These works lead towards a possible image analysis based damage descriptor for corrosion, where the corroded regions are optically in contrast with their respective surroundings. Since metal ions, in the presence of water, oxygen and/or organic and inorganic acids in the marine environment tend to form coloured products, the discolouration due to corrosion is usually common. This fact has been observed by Tsushima et.al (1997) in conjunction with basic image processing methodology. Chemical treatment of the corroded samples in the laboratory usually brings about such contrast.

On the other hand, the effects of an NDT method on the long term goal of structural maintenance and optimized management have been discussed by Rouhan and Schoefs (2003) in an example on offshore structures. The role of the probability of detection (PoD) and the probability of false alarm (PFA) in a maintenance strategy are discussed. Recently it has been extended for stochastic fields of uniform corrosion by Schoefs et al. (2007). Vibration based identification of damage in bridge structures and the relationship associated only with PoD have been discussed by Alvandi and Cremona (2006) very recently where the relative ranking of various NDT methods have been emphasized. Study on pitting corrosion in aircraft wings have been related to NDT

probabilistically by Harlow and Wei (1999). Zheng and Ellingwood (1998) have illustrated uncertainty characterization of NDT techniques related to condition assessment of structures.

It is thus felt that there is a definite scope and necessity of connecting the probabilistic information based relative ranking of NDT tools under various environmental conditions in conjunction with damage definition based human interpretation of the consequences of damage in structures in a case specific manner. In this paper, an image processing based damage detection tool has been considered as the chosen NDT. Photographs of various qualities due to the change of environmental factors have been considered for the purpose of identification considering two alternate definitions of damage. The applicability of the NDT tool has been quantified and a sensitivity study has been performed probabilistically to identify the important external conditions and their relative effects on the detection process.

2. IMAGE PROCESSING BASED DAMAGE DETECTION

2.1 Image Dependant Information

The measurement of the quantitative aspects of corrosion is extremely difficult for an underwater structure like steel piles. However, information based on the photographs of the corroded regions can be made available using techniques related to image processing. These photographs can come directly from the piles or can be from experimental plates attached to the piles or those corroded in a similar environment within the laboratory. The corroded plates can be untreated or chemically treated to accentuate the corroded region. A successful identification of the presence, location and

extent of damage using such photographs is required by any structural health monitoring scheme. In order to better assess the calibration parameters under controlled conditions, a case of pitting corrosion on experimentally corroded plates is chosen. Figure 1 shows an example of one of the treated plates. The sample is an aluminium plate immersed in an aluminium tank for 20 years within the mud zone of a lake very close to the sea near the St-Nazaire harbour in cold brackish water. Aluminium is very sensitive to pitting corrosion, especially in chloride containing environments and the damaged condition can thus be achieved.

The corroded regions are observed to be in contrast with the background and this fact is considered to be the starting point behind damage detection from photographic information. Even when the damage samples are available, both from the laboratory and from the structure, the quantification of the damage is manual and hence difficult and time consuming task. As a result such assessments are usually limited to accurate identification of the presence of damage. The information of the geometric properties of the damage are less reliable due to the presence of human factor and the time involved with such analyses increase greatly even when the number of observations is moderate in size. All these problems necessitate the development of an image processing based damage detection technique that is easy to handle, more accurate and less time consuming.

2.2 Theoretical Background and Detection Scheme

The detection method in this paper considers that the damage regions present in the photograph are optically different from their surroundings in terms of colour, brightness and geometry. The objective is to convert the coloured image to a binary image and

identify the edges of the damaged regions successfully. A successful detection ensures that the coordinates of all the points lying at the edge of the closed geometry of the damages are available. By calibrating the pixel length of the photographs in the horizontal and the vertical direction against some pre-existing benchmark of distance in the real specimen or structure, the entire spatial geometry of the damaged regions are retrieved along with the possibility of post- processing to obtain the statistical measures of such geometry. The MATLAB image processing toolbox (MATLAB, 2006) has been employed for the proposed detection scheme. The efficiency of the detection lies in the contrast of the damage region with respect to its surroundings and the ability of the analyzing system to identify such contrasts within a closed geometry. An example of this detection is given in Figure 2, where Figure 1 has been successfully analyzed to isolate eight major closed damaged areas of irregular geometry. Some spurious features are also identified due to the environmental noise but are insignificant with respect to the damaged regions. The size of the spurious features is related to false alarm and can be connected with the predefined size classification of different damages. This classification must be related to the use of false alarm in the maintenance policy as shown by Schoefs and Clement (2004). Such detection processes can be helpful for the structural health monitoring and assessments of actual structures. The efficiency of the detection depends heavily on the quality of the available information. Figures 3a and 3b are presented in this regard where a frame of a basic structural inspection (visual) and reconnaissance video of the steel piles of the harbour of St. Nazaire has been frozen and analysed to identify the possible major damage locations. Distributed discoloration on the piles due to chemical action is observed in the image (Figure 3a). Figures 3a and 3b illustrate the fact that the

quality of an image analysis based structural health monitoring and assessment technique heavily depends on the quality of the obtained image.

2.3 Statistical Information

Once the closed geometries and their co-ordinates are identified within the photograph, various statistical properties of the geometries can be found. The centroids, the areas within each identified object and the major and minor axes of each of the objects have been computed in this study as an example using the MATLAB image processing toolbox. The summary of the information is provided in Table 1 where the spatial variability and the extent of the damage regions have been quantified. Any other photograph produces such results and can be related to the actual length scale by choosing a pre-existing benchmark.

It is also important to note that the objects labelled 2 and 3 in Figure 2 are considered to be a single object while processing and hence the combined geometric property of the system has been rendered instead of their individual statistics. This is due to the fact that in the real specimen the damages are in fact physically connected. However, by a proper control on preprocessing, lighting and camera resolution these two geometric regions can be separated incorporating some additional effort.

The information provided by Table 1 can also acts as a tool for the relative ranking of the damaged locations within the structure. For this particular case the total area of damage has been found to be approximately 5.7% of the total area under consideration. The unit of length in Table 1 is in pixels and that of area is in square pixels. The terms Xbar and Ybar represent the coordinates of the centroids of each labeled damaged region in horizontal and vertical direction respectively. With the information on the successful

detections and false alarms available, the receiver operating characteristics can be constructed.

3. PROBABILISTIC STUDY ON IMAGE PROCESSING BASED DAMAGE DETECTION AND CALIBRATION

3.1 Inspection Results Modeling: Basic Theoretical Concepts.

Applications of image processing have gained popularity very recently in the field of structural health monitoring. Patsias & Staszewski (2002) have illustrated that inspection using video processing is not perfect when considering on site video recording. Luminosity, noise and contrast are quite different from one photograph to the other.

It has thus become a common practice to model the detection reliability in terms of the probability of detection (PoD), the probability of false alarms (PFA) and the Receiver Operating Characteristic (ROC) curves. The most common concept which characterizes inspection tool performance is the probability of detection. Here the PoD depends on the maximum size of the defect and the area of the defect and the PFA depends on the noise and the detection threshold. For simplicity, we can consider the area of pitting to be a governing parameter involved in the damage process which can be related to the consequence or decision making directly. Let A_d (detection threshold) be the minimal pitting area under which it is assumed that there is no detection. Thus, the probability of detection is defined as

$$\mathrm{PoD}(A) = \mathrm{P}(A \geq A_d) \qquad (1)$$

where A is the measured area and A_d is a deterministic parameter or a random variable. This definition implies that PoD is a monotonic increasing function. To complete this concept, the probability of false alarm is devoted to deal with the detection of non existing defects. In view to introduce these concepts into practicable decision schemes, recent works have been carried out (Rouhan and Schoefs (2000) and (2003)).

3.2 Statistical Modelling of Inspection Results

Knowing the probability density functions (pdf) of the signal and noise and that of the noise alone, the computation of PoD and PFA can be performed easily (Rouhan & Schoefs (2003)). In practice, there is actually no way to obtain the pdf of a signal and the signal and noise together for image processing in harsh conditions where many factors affect the inspection results. One way of modelling such parameters is to analyse the probabilistic structure of the inspection results and to provide a model consequently. The I.C.O.N (Rudlin & Dover 1996, Barnouin et al. 1993) project has been dedicated to the inter-calibration of the N.D.T tools with the appropriate checks done on-the-spot in recent times for this purpose.

The image analysis based damage classification procedure conforms to such probabilistic information structure. We assume that every correctly detected defect has a proper and identifiable shape and can be related to a certain PoD based on how closely the extent of damage has been identified once the damage region is detected. On the other hand, the PFA is related to identifying a spurious region larger than a predefined threshold above which damage is considered significant. In this study we do not rank the defects with a given classification to assess the PoD within a given range. Rather, the aim

is to assess the PoD for the whole range of observed defects. Accordingly, the PoD and PFA are defined as

$$\mathrm{PoD} = \frac{\left| \sum_{i=1}^{n} \bar{A}_i - \sum_{i=1}^{n} A_i \right|}{\sum_{i=1}^{n} \bar{A}_i} \tag{2}$$

$$\mathrm{PFA} = \frac{n_s}{n_t} \quad \text{where} \quad A_s \geq A_{th} \tag{3}$$

where $\bar{A}_i$ is the actual extent of damage in the i^{th} damaged region, A_i is the measured extent of damage in the i^{th} damaged region, A_s is the measured extent of damage in a region where damage does not exist and A_{th} is the threshold of the extent of damage beyond which the damage is termed significant. The actual extent of the damage $\bar{A}_i$ is usually an ideal condition achieved by a health monitoring and assessment technique and is not usually available to the engineer a-priori. However, this factor establishes the reference value for the actual damage, and thus in turn affects the effectiveness of the technique. Laboratory based, simulation based and benchmarking based studies can be effective for the establishment of the parameter $\bar{A}_i$, the first two methods being comparatively much cheaper, rapid and more accessible than a full scale benchmarking. The factor A_i is the direct processed output of any assessment or evaluation method is usually available and must be compared with the established $\bar{A}_i$ value. While a source of error from the measurements can be related to the error is quantifying the damage, there also exists another source of error for any assessment technique in terms of identifying a damage where no damage exists, thus giving rise to false alarms. A typical example related to the present paper can be regions where due to some spurious colour contrast

zone clustering, the image processing based identification demarcates closed geometries which are not damaged at all. If the sizes of the wrongly identified closed geometries are larger than a preselected size of the damage condition, then it is counted as a false alarm. The preselected threshold size of damage can be from mechanical conditions or from serviceability constraints or other constraints (including aesthetics) arising both from the engineer and the clients' requirement. The parameters n, n_s and n_t denote the total number of correctly identified damage regions, the total number of spuriously identified damage regions and the net total number of identified damage regions (both correct and incorrect) respectively.

For all practical cases, the deviation of the extent of the measured detected damaged region does not go beyond 100% of the actual extent of the damaged region and thus equation 2 can be considered to be consistent for real life situations. On the other hand, any spurious but significant detection will warrant a test or a check at a place where no damage is present. Thus, the size of detection does not matter in the case of PFA once the threshold/s of significant damage is/are defined.

The damage is defined from two different viewpoints, one based on the total area of the damaged region and the other based on the major axis of the damaged region. Sometimes the area of the damage is not large but the major axis can be large enough to have significant effects on the structure. Under those circumstances, significant change of result can be expected.

4. RECEIVER OPERATING CHARACTERISTICS (ROC) AND THE ISOLATION OF OPERATING CONDITIONS

4.1 Damage Identification for Various Operating Conditions

The quality of the photograph (Figure 1) is assumed to be chiefly affected by luminosity, contrast and noise. This corresponds to the on-site parameters which affect the quality of submarine pictures. In this paper, three different levels (high, normal and low) of each of such affecting factors have been chosen and the effects of such change on the photograph are shown is Figure 4. The additive Gaussian noise has been characterised by its parameters of the normal distribution and can be introduced through MATLAB image processing toolbox. The luminosity is changed by changing the amount of 'whites' in each pixel while the contrast change can be characterized by tuning the differences between the adjacent colours in each pixel. This can be obtained easily through commercial photo editors, where the luminosity and contrasts are usually marked within a scale of zero to hundred. The nomenclature followed for each of such realisation of external condition is provided in Table 2. It is clearly observed that certain combinations of luminosity, contrast and noise pose a much greater difficulty in terms of correct identification and estimation of the damage extent than others.

An image is essentially a rectangular grid of pixels and the centre of a pixel occupies the integer co-ordinates in the grid so produced. The interior of each pixel can be further subdivided into a continuous spatial coordinate system also by considering that the local origin for each pixel lies at the top left hand corner of the pixel. Each pixel is associated with a vector of number describing its hue-saturation value. The grey-level

threshold of the image is computed by minimizing the interclass variances of the black and white pixels using Otsu's method using MATLAB 7.0 image processing toolbox (MATLAB, 2006). The method is also used in the field of computer vision and is aimed at separating the foreground from the background. Pixels below the threshold assume a value zero and turn black, while the other pixels turn white. This enables to convert a complex matrix from the original image to a simpler binary black and white image. This transformation is important when the feature of interest is in contrast with its surroundings in the image. However, the automatically computed grey-level threshold does not turn out to be the best for appropriate detection of damaged region in the image for the present study and certain adjustments of the threshold were carried out to obtain the best possible information from the post-processing of the existing image. This is because of the fact that the identification of damaged regions or the regions of interest is essentially a local and image specific phenomenon on the two-dimensional photographic plane and thus the maximisations of the interclass variances in the sub-regions of interest is not always possible. A possible solution to this problem is to incorporate a correction to the grey-level threshold and heuristically find the best value of the threshold maximising the visual information of the picture in terms of damage identification. Figure 5 illustrates the adjustments of the grey-level threshold required for various images corresponding to various environmental conditions. The non-adjusted threshold values refer to that obtained from Otsu's method, while the adjusted values correspond to the values obtained from heuristic thresholding. It is important to note here that for certain conditions, the heuristically set best thresholding can be significantly different

from that obtained by Otsu's method. The corresponding improvement in each of the images for such re-adjustment has been qualitatively presented in Table 3.

4.2 Effects of the Damage Descriptors

The ROC for different quality of images can be constructed and interpreted based on the parameter incorporated to define and describe the damage. In the present study, two alternative definitions of damage using the damaged area and the major axis of the damaged area as descriptors are presented. The ROC based on the area dependent damage and the major axis dependent damage are respectively presented in Figures 6a and 6b along with the improvement after the readjustment of grey-level threshold. Figure 6 illustrates the fact that the area based identification is more appropriate in the current situation rather than the major axis based identification, as is reflected by the consistent POD-PFA scatter, where most of the points belong to the domain of high efficiency. On the other hand, Figure 6 allows observing the improvement after re-adjusting the grey-level threshold on a quantitative term. The effect is quite pronounced in Figure 6b where more number of points enter a considerably higher domain of efficiency. The area based damage detection is thus found to be suitable in the present case and the ROC based on the damage definition using major axis is observed to have a comparatively higher spread. The improvement of the ROC after readjustment of the grey-level threshold is found to be pronounced in the case of a major-axis based damage detection as well. Many of the images are found unsuitable for a damage definition based on major axis even though these are suitable for a definition based on area. The effect of damage descriptors for defining the damage extent on the efficiency of the NDT method is thus illustrated .

4.3 Effects of Environmental Parameters and Isolation of Operating Conditions

The sensitivity of each affecting environmental parameter for ROC has been investigated in details for different damage definitions and improvement of image by post processing. Under these conditions it is easier to isolate the dominant environmental effects and effects that can be improved. Figures 7a (area based sub-classification) and 7b (major axis based sub-classification) illustrate this. The POD-PFA scatter has been plotted in terms of environmental sub-classifications in this figure. The non-adjusted and the adjusted grey-level thresholding conditions have been marked in the legend as 'O' and 'N' respectively. The interactions between pairs of environmental parameters are presented in each of the figures respectively while the third parameter is kept at its normal level. For example, the first sub-graph of Figure 7a investigates the interaction between normal luminosity for various levels of contrast in the presence of normal noise for both adjusted and non-adjusted cases. These parametric investigations help identifying, classifying and prioritizing the important combinations of environmental factors on the quality of an assessment technique. The presence of high noise is found to be a major deterrent in terms of damage identification in the present case for both major axis based and area based representation while the combination of high luminosity in conjunction with high contrast is not recommended either. Low noise and normal luminosity are found to be preferable operating conditions for the present case. Low and normal contrast conditions are preferable since the discoloration of the damaged region is

significant. However, these conditions can pose a difficulty to the detection process if the discoloration merges with the surroundings with a change in contrast, thus masking the actual damage region. Table 4 provides the PoD-PFA values for the twenty seven cases investigated for various environmental conditions. The terms ‘old’ and ‘new’ refer to the non-adjusted and the adjusted grey-level thresholds respectively. A first measure of the quality of a NDT from ROC can be defined to be the distance between the ideal inspection with coordinates (PFA=0;PoD=1) and the point of the ROC under consideration for a site-specific condition assessment regime. This approach can be improved with the knowledge of the maintenance policy within the structural health monitoring framework in terms of repair, maintenance and new inspection along with the binary (detection or not) inspection results. The isolation of the operating conditions can thus be directly related to an improvement in the general damage detection process.

5. CONCLUSIONS

The paper illustrates the isolation of suitable events for structural health monitoring for a specific NDT tool from a large number of outcomes to maximize the receiver operating characteristic of such tool. An image processing based damage classification methodology to identify corrosion has been used and the subjectivity of the image based method has been emphasized. The possibility of improvement of the detection process of an NDT through post processing of acquired data is illustrated through an example. The effects and the relative importance of environmental parameters affecting the detection process have identified and the quantification of sensitivity has been achieved through the

ROC curves. The illustrated methodology is very general and provides with a case specific construction of ROC. The importance of the definition of damage and interpretation of the consequences of it, i.e. the limit state has been observed. This general methodology can be used for any NDT tool by practicing professionals as a guideline for choosing conducive events for structural health monitoring and damage detection, prioritizing and ranking the major affecting environmental factors and estimating and case specific quantification of the efficiency of such NDT. In terms of application to the maintenance of harbors, the choice of better environmental conditions and video devices can help achieve a better ROC under current conditions and recommend a practical guideline defining the on-site protocol. On the other hand, the methodology provides a calibrated ROC to analyze the risk of wrong assessment using the result of image processing when the measurements of a set of simple environmental conditions are available.

REFERENCES

1. SAMARIS. Sustainable and Advanced MAterials for Roads InfraStructures, Research program financed by European Community founds, http://samaris.zag.si, december 2002-november 2005.
2. Schoefs F. et Clément A. (2004). "Multiple inspection modelling for decision making and management of jacket offshore platforms: effects of False Alarms". First International Forum on Engineering Decision Making (IFED'04), december 5-9 2004, Stoos, Switzerland (2004).
3. Patsias S and Staszewski W J. (2002). "Damage Detection using Optical Measurements and Wavelets", Structural Health Monitoring, Vol 1(1), 5-22.
4. Rucka M and Wilde K. (2006). "Crack Identification using Wavelets on Experimental Static Deflection Profiles", Engineering Structures, 28, 279-288.
5. Hartman A M and Gilchrist M D. (2004). "Evaluating Four-Point Bend Fatigue of Asphalt Mix Using Image Analysis", ASCE Journal of Materials in Civil Engineering, January-February, 60-68.
6. Gehle R W and Masri S F. (1998). "Tracking the Multi Component Motion of a Cable using a Television Camera". Smart Materials and Structures, 7, 43-51.
7. Benning W, Lange J, Schwermann R, Efkemann C and Gortz S. (2004). "Monitoring Crack Origin and Evolution at Concrete Elements Using Photogrammetry". XXth ISPRS Congress, Commission V, Istanbul, Turkey.

8. Barinova L and Pospisil J. (2002). “Computer Image Analysis of the Human Mouth Shape”. ACTA Univ. Palacki. Olomuc, FAC.RER.NAT. (2001-2002), Physica 40-41, 163-173.

9. Rouhan A and Schoefs F. (2003). “ Probabilistic Modelling of Inspection Results for Offshore Structures”. Structural Safety, 25, 379-399.

10. Schoefs F., Clément A., Memet J.B., and Nouy A. (2007). “Spatial dependence of Receiver Operating Characteristic curves for Risk Based Inspection of corroded structures: application to on-pile wharf”, to be published in the Proceeding of 10th international conference on Applications of Statistics and Probability in Civil Engineering, (I.C.A.S.P’07), July31-August 3 2007, Tokyo, Japan, pp. ?, 8 pages.

11. Rudlin JR, Dover WD. (1996). “The ICON database. Assisting underwater inspections”. In: Offshore technology, vol. 4.

12. Barnouin B., Lemoine L, Dover W.D., Rudlin J., Fabbri S., Rebourcet G., Topp D., Kare R., Sangouard D. (1993). “Un-derwater inspection reliability trials for offshore structures”. In ASME NY, editor. Proc. of the 12th International Con-ference on Offshore Mechanics and Arctic Engineering. Vol. 2 pp. 883-890.

13. Alvandi A and Cremona C. (2006). “Assessment of Vibration-based Damage Identification Techniques”. Journal of Sound and Vibration, 292, 179-202.

14. Harlow D G and Wei R P. (1999). “Probabilities of Occurrence and Detection of Damage in Airframe Materials”. Fatigue Fract Engng Mater Struct, 22, 427-436.

15. Zheng R and Ellingwood B R. (1998). “Role of non-Destructive Evaluation in Time-Independent Reliability Analysis”. Structural Safety, 20, 325-339.

16. Rouhan A, Schoefs F. 2000. On the use of inspections results, in IMR plans. In: Mangin MM, editor. DMinUCE—2000. Second International Conference on decision making in urban and civil engineering, vol. 2, p. 1259–70.

17. Rouhan A., Schoefs F. 2003. Probabilistic modelling of inspection results for offshore structures, Structural Safety, vol 25, pp. 379-399, 20 pages, (Elsevier Ltd. 2003)

18. Tsushima T., Ishii A., Ochi Y., Masaoka N and Matsusue H. (1997). “Corrosion Inspection of Steel Tube Inner Wall”. IEEE/ASME International Conference on Advanced Intelligent Mechatronics ’97, Final Program and Abstracts (Cat No. 97TH8298), 34-34.

19. MATLAB. (2006). "Image Processing Toolbox". The Mathworks Inc., 3 Apple Hill Drive, Natick, MA, USA.

LIST OF FIGURES

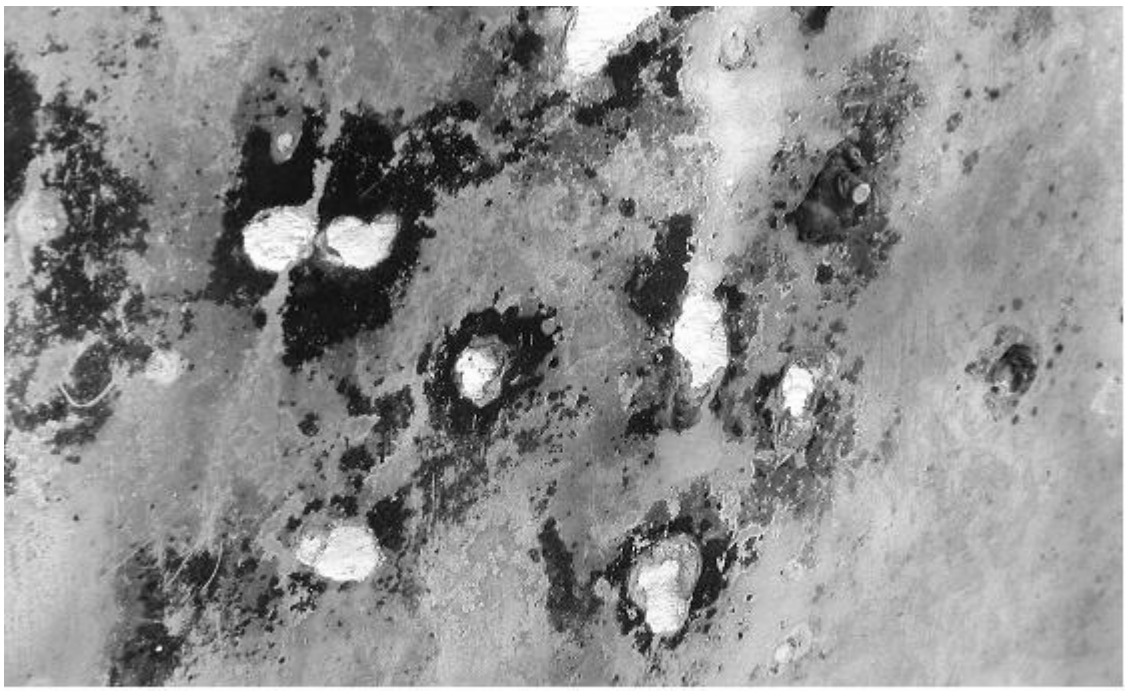

Figure 1.

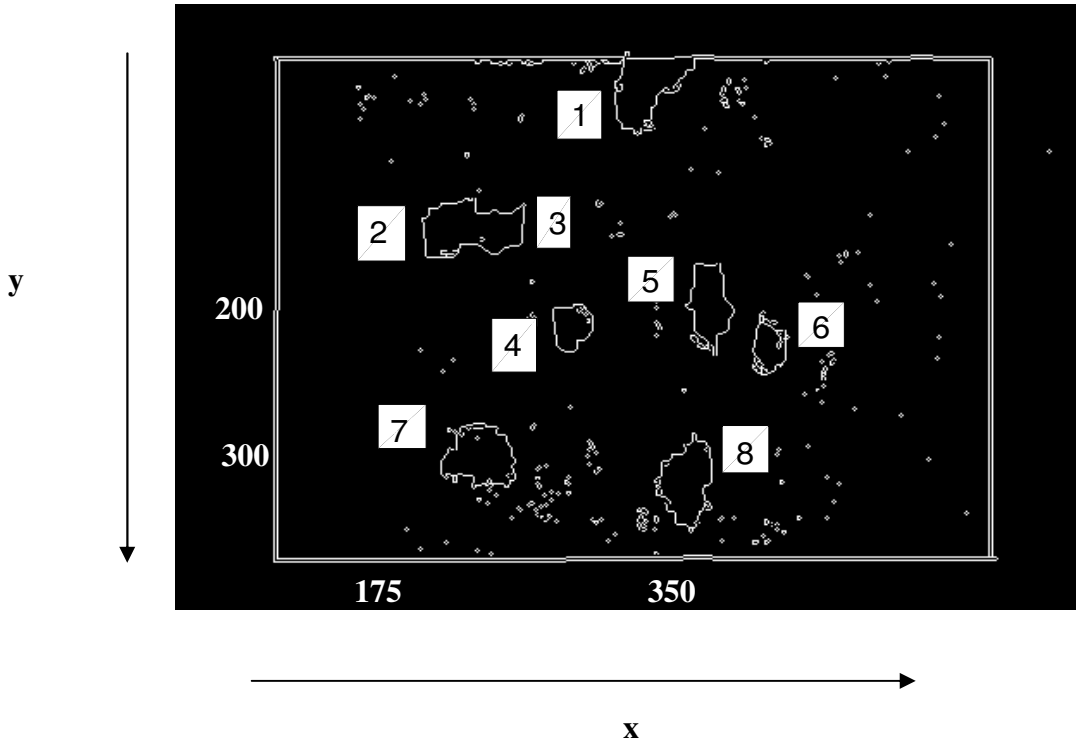

Figure 2.

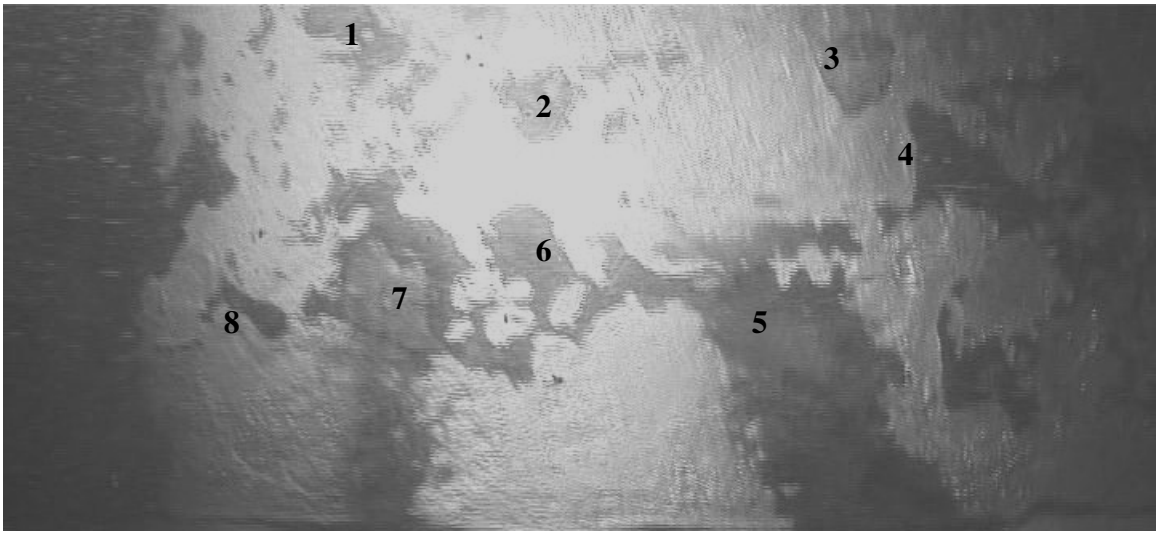

Figure 3a.

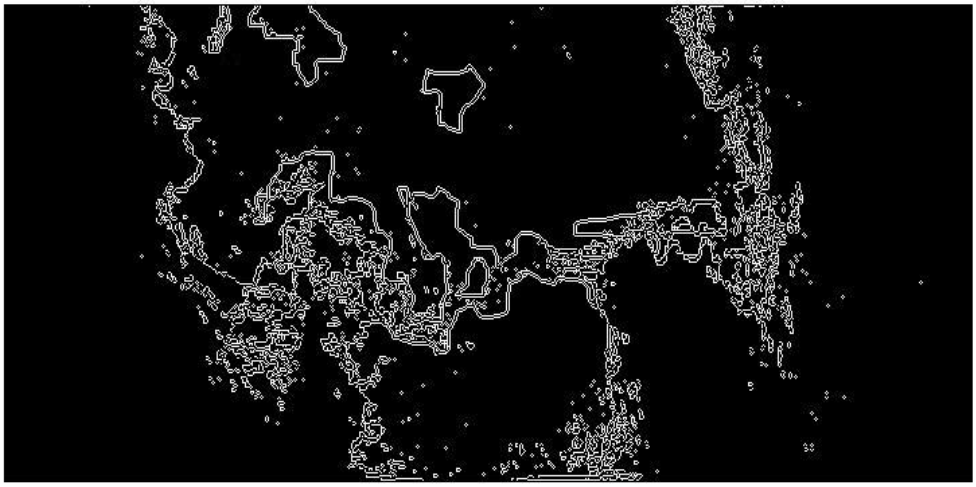

Figure 3b.


1


2

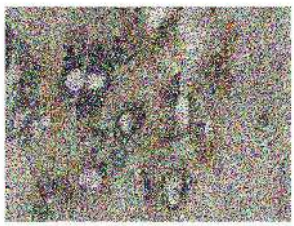
3


4


5

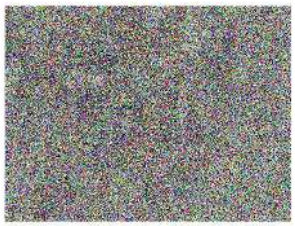
6


7


8


9

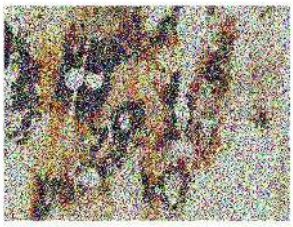
10


11


12


13


14

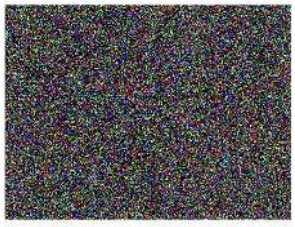
15


16


17

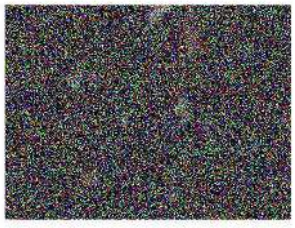
18

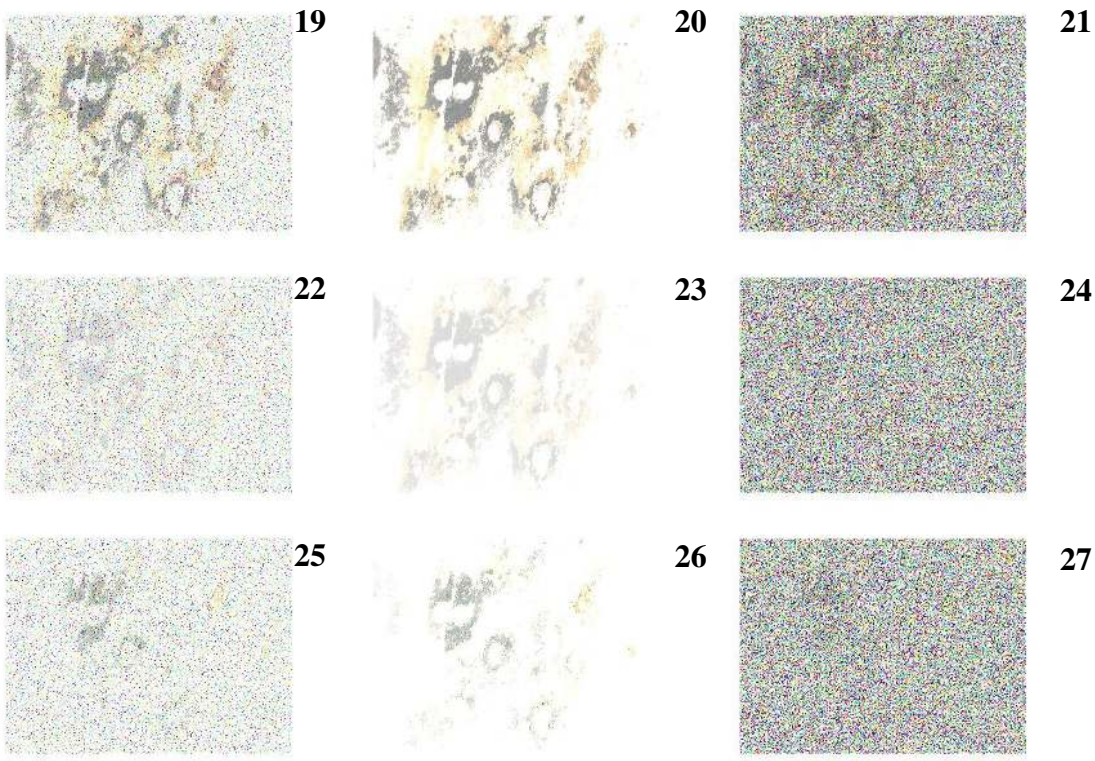

Figure 4.

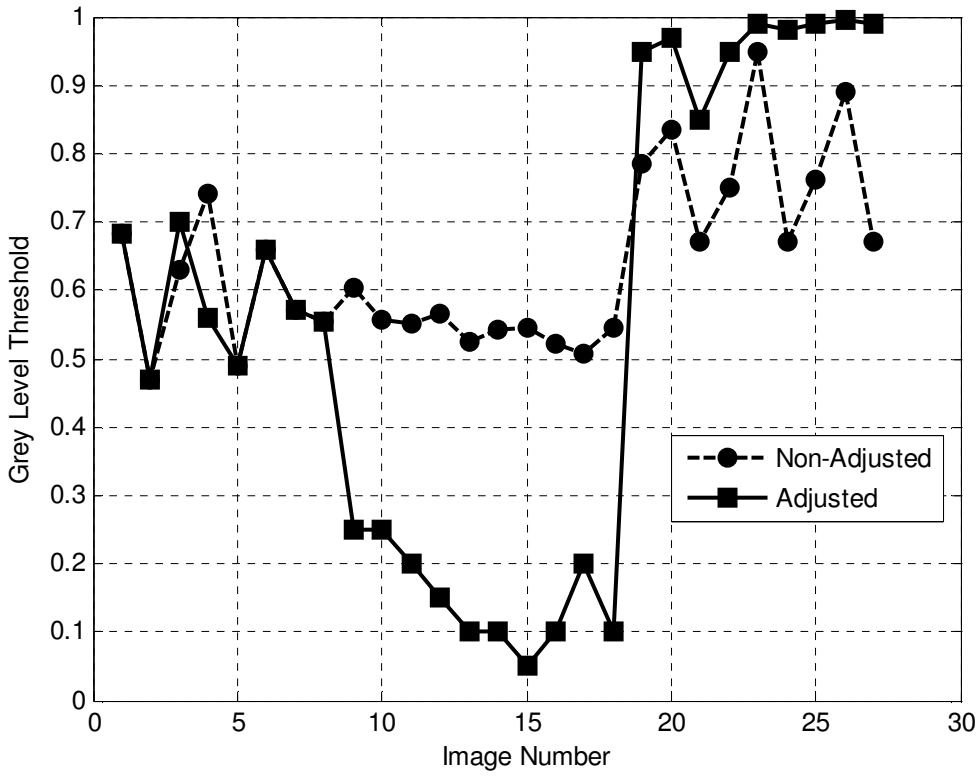
Grey Level Threshold
Image Number
Non-Adjusted
Adjusted
0
0.1
0.2
0.3
0.4
0.5
0.6
0.7
0.8
0.9
1
0
5
10
15
20
25
30

Figure 5.

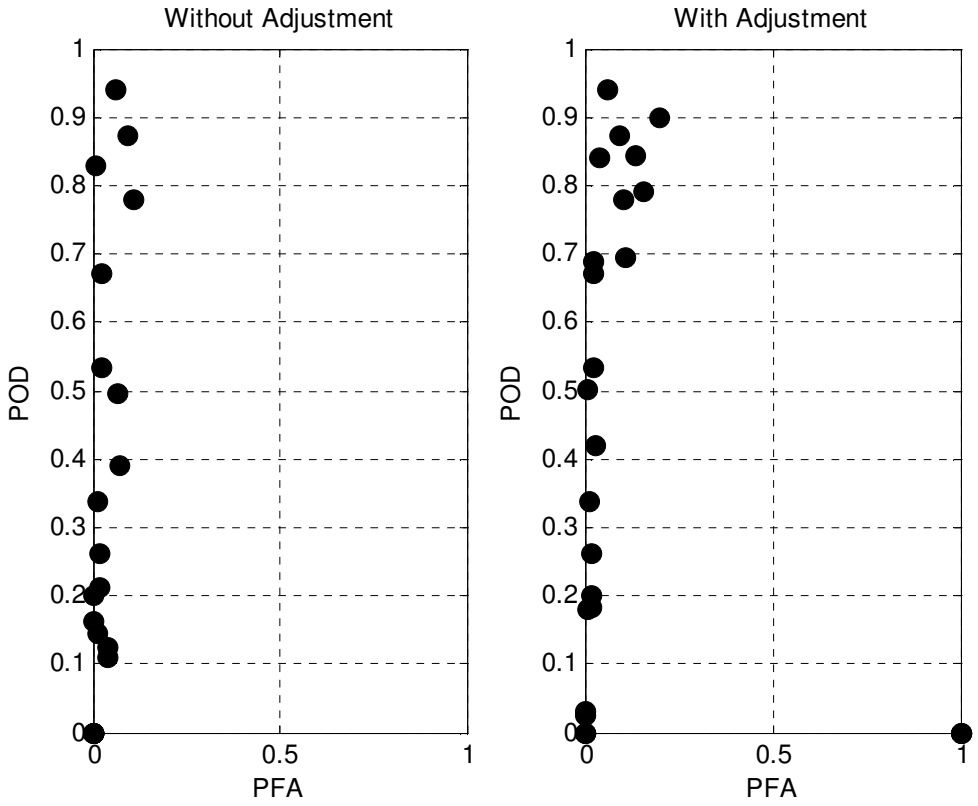
Without Adjustment
With Adjustment
POD
PFA
0
0.1
0.2
0.3
0.4
0.5
0.6
0.7
0.8
0.9
1
0.5

Figure 6a.

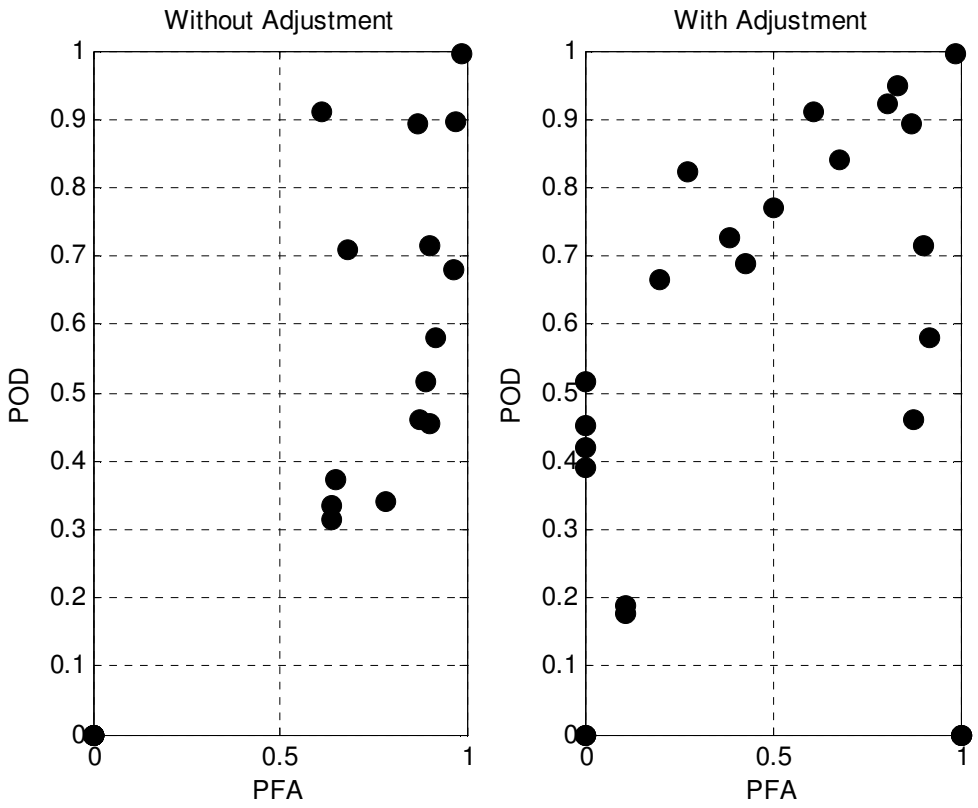
Without Adjustment
With Adjustment
POD
PFA
0
0.1
0.2
0.3
0.4
0.5
0.6
0.7
0.8
0.9
1
0.5

Figure 6b.

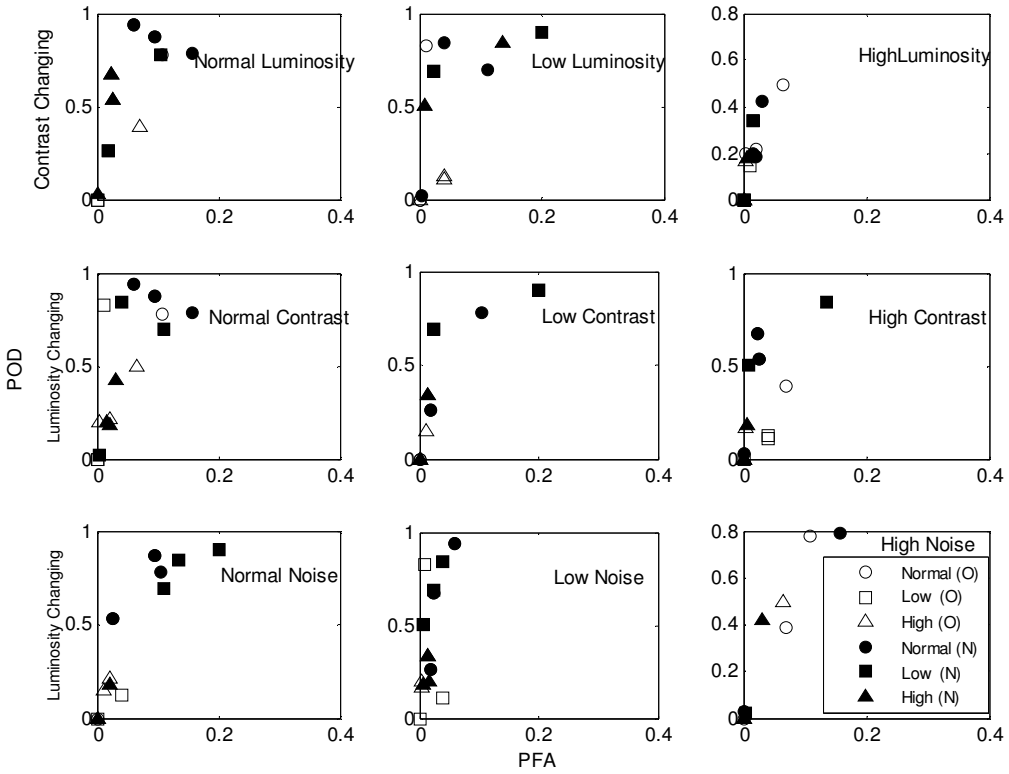
Contrast Changing
Normal Luminosity
Low Luminosity
HighLuminosity
POD
Luminosity Changing
Normal Contrast
Low Contrast
High Contrast
Luminosity Changing
Normal Noise
Low Noise
High Noise
Normal (O)
Low (O)
High (O)
Normal (N)
Low (N)
High (N)
PFA

Figure 7a.

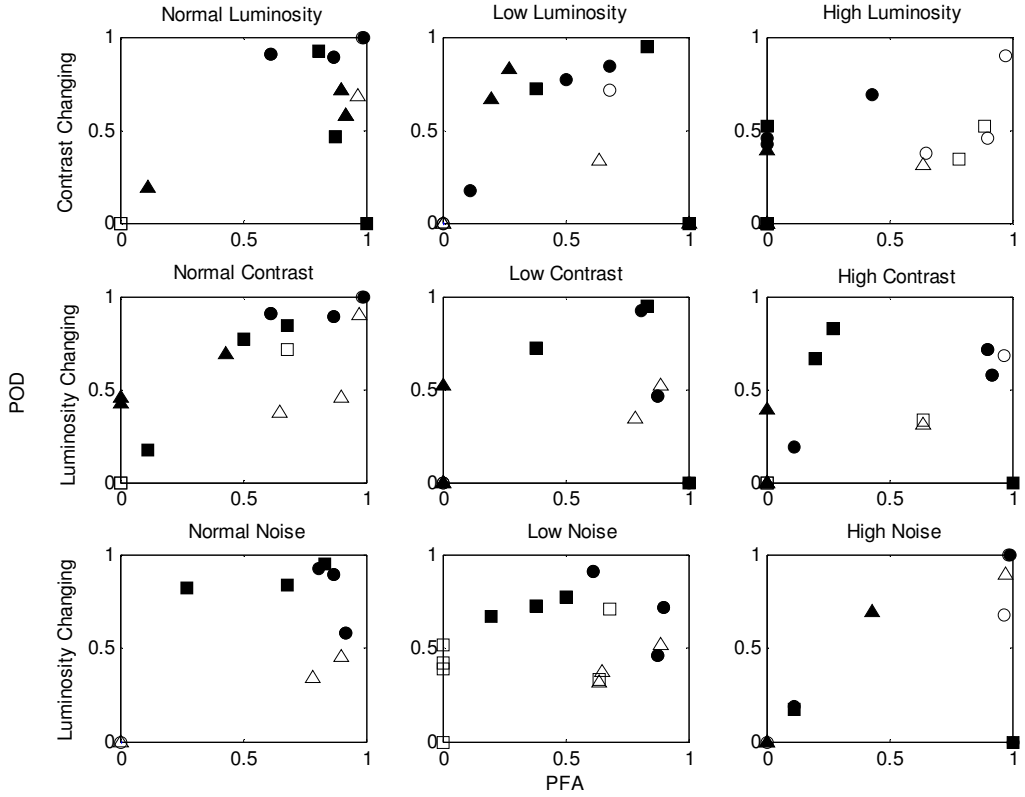
Normal Luminosity
Low Luminosity
High Luminosity
Normal Contrast
Low Contrast
High Contrast
Normal Noise
Low Noise
High Noise
Contrast Changing
Luminosity Changing
Luminosity Changing
POD
PFA
0
0.5
1

Figure 7b.

LIST OF TABLES

Damage No.	Xbar	Ybar	Major Axis	Minor Axis	Area	% Area
1	273	56	51	36	1151	0.9
2 &3	173	139	66	34	1597	1.25
4	232	200	30	24	539	0.42
5	311	186	56	24	985	0.77
6	346	212	34.5	20.3	494	0.38
7	178	280	44	39.4	1272	0.99
8	298	295	54	31.2	1240	0.97

Table 1.

		Quality		
Image Number	**Luminosity**	**Contrast**	**Noise**	
1	Normal	Normal	Normal	NNN
2	Normal	Normal	Low	NNL
3	Normal	Normal	High	NNH
4	Normal	Low	Normal	NLN
5	Normal	Low	Low	NLL
6	Normal	Low	High	NLH
7	Normal	High	Normal	NHN
8	Normal	High	Low	NHL
9	Normal	High	High	NHH
10	Low	Normal	Normal	LNN
11	Low	Normal	Low	LNL
12	Low	Normal	High	LNH
13	Low	Low	Normal	LLN
14	Low	Low	Low	LLL
15	Low	Low	High	LLH
16	Low	High	Normal	LHN
17	Low	High	Low	LHL
18	Low	High	High	LHH
19	High	Normal	Normal	HNN
20	High	Normal	Low	HNL
21	High	Normal	High	HNH
22	High	Low	Normal	HLN
23	High	Low	Low	HLL
24	High	Low	High	HLH
25	High	High	Normal	HHN
26	High	High	Low	HHL
27	High	High	High	HHH

Table 2.

	Quality			Level of Identification	
Image Number	**Luminosity**	**Contrast**	**Noise**	**Without Threshold Adjust ment**	**With Threshold Adjustment**
1	Normal	Normal	Normal	Somewhat	Somewhat
2	Normal	Normal	Low	Somewhat	Somewhat
3	Normal	Normal	High	Somewhat	Somewhat
4	Normal	Low	Normal	Good	Good
5	Normal	Low	Low	Somewhat	Somewhat
6	Normal	Low	High	None	None
7	Normal	High	Normal	Good	Good
8	Normal	High	Low	Good	Good
9	Normal	High	High	Somewhat	Good
10	Low	Normal	Normal	None	Good
11	Low	Normal	Low	None	Good
12	Low	Normal	High	None	Somewhat
13	Low	Low	Normal	None	Good
14	Low	Low	Low	None	Good
15	Low	Low	High	None	Poor
16	Low	High	Normal	None	Good
17	Low	High	Low	Somewhat	Good
18	Low	High	High	None	Somewhat
19	High	Normal	Normal	Somewhat	Good
20	High	Normal	Low	Somewhat	Good
21	High	Normal	High	None	Somewhat
22	High	Low	Normal	None	Somewhat
23	High	Low	Low	Somewhat	Good
24	High	Low	High	None	None
25	High	High	Normal	None	None
26	High	High	Low	Somewhat	Fairly Good
27	High	High	High	None	None

Table 3.

Case	POD				PFA			
	Area Based		Major Axis Based		Area Based		Major Axis Based	
	Old	New	Old	New	Old	New	Old	New
1	0.8714	0.8714	0.8942	0.8942	0.0943	0.0943	0.8689	0.8689
2	0.94	0.94	0.91	0.91	0.06	0.06	0.61	0.61
3	0.78	0.79	0.9969	0.995	0.1079	0.1578	0.984	0.989
4	0	0.7782	0	0.9212	0	0.104	0	0.8049
5	0.2606	0.2606	0.46	0.46	0.018	0.018	0.877	0.877
6	0	0	0	0	0	1	0	1
7	0.533	0.533	0.58	0.58	0.0264	0.0264	0.9192	0.9192
8	0.67	0.67	0.7153	0.7153	0.023	0.023	0.9	0.9
9	0.39	0.03	0.68	0.19	0.07	0.0017	0.964	0.11
10	0	0.6939	0	0.84	0	0.111	0	0.68
11	0.83	0.84	0.71	0.77	0.01	0.04	0.68	0.5
12	0	0.024	0	0.176	0	0.0025	0	0.111
13	0	0.9	0	0.95	0	0.2	0	0.83
14	0	0.69	0	0.7253	0	0.0231	0	0.384
15	0	0	0	0	0	1	0	1
16	0.124	0.8425	0	0.8228	0.04	0.135	0	0.2727
17	0.1083	0.5004	0.334	0.6643	0.04	0.0074	0.64	0.2
18	0	0	0	0	0	1	0	1
19	0.213	0.183	0.4534	0.453	0.02	0.02	0.9	0
20	0.2	0.2	0.3721	0.42	0.0042	0.017	0.65	0
21	0.4957	0.42	0.8956	0.69	0.0642	0.0317	0.97	0.43
22	0.1443	0	0.34	0	0.011	0	0.7838	0
23	0.3372	0.3372	0.5173	0.5173	0.015	0.015	0.89	0
24	0	0	0	0	0	0	0	0
25	0	0	0	0	0	0	0	0
26	0.1635	0.18	0.3136	0.39	0.004	0.007	0.6364	0
27	0	0	0	0	0	0	0	0

Table 4.